Progress In Electromagnetics Research M, Vol. 120, 83–94, 2023

High-Eccentricity Orbit Synthetic Aperture Radar with Multi-Parameters Joint Agile Variation

Xuhang Lu[1, 2, *], Wei Xu[1, 2], Pingping Huang[1, 2], Weixian Tan[1, 2], and Yaolong Qi[1, 2]

Abstract—The variable orbit altitude and platform velocity in high-eccentricity orbit synthetic aperture radar (HEO SAR) increase the difficulty in obtaining effective radar echoes. In this paper, a new stripmap imaging mode with multi-parameter joint agile variation in HEO-SAR is proposed. First, the range sidelooking angle is adjusted during the whole raw data acquisition interval according to the time-varying side-looking geometric relationship, while the pulse repetition frequency (PRF) is continuously changed to obtain uniform azimuth sampling due to the satellite velocity variation. Besides simultaneously adjusting the side-looking angle and the operated PRF, echo sampling start time and range sampling points are also continuously changed to decrease the echo data rate. According to the echo characteristics in HEO SAR, its corresponding imaging algorithm is presented, which includes range samples adjustment, azimuth resampling, cubic filtering, nonuniform Fourier fast transform (NUFFT) for nonlinear range cell migration correction (RCMC) and modified azimuth compression. A system design example with multi-parameters joint agile variation for the desired resolution of 3 m and the swath width of 30 km is given, while imaging simulation experiments on point targets are carried out. Both simulation results of multi-parameters variation design and point targets imaging validate the proposed stripmap imaging mode with multi-parameters joint agile variation in HEO SAR.

1. INTRODUCTION

Spaceborne synthetic aperture radar (SAR) is a pioneering technology offering unrivaled possibilities for earth observation, capable of providing high-resolution imagery irrespective of weather conditions or daylight availability. Resolution and swath width represent two critical imaging technical indices in SAR, consistently forming the crux of ongoing research endeavors and technological advancements. To achieve high-resolution imaging, it is typically necessary to make full use of the radar system's capabilities, which are more readily accomplished at lower orbital altitudes as this enables the maximization of the observational efficiency of the SAR system. Conversely, achieving a wider swath generally becomes more feasible at higher orbital altitudes, as this facilitates broader coverage and reduces the frequency of satellite revisits.

SAR imaging using satellites in high elliptical orbits can provide high-resolution wide-swath images and has drawn extensive research interests [1, 2]. A bistatic SAR system with a geosynchronous satellite transmitter and a low earth orbit receiver was designed [3], and an overlapped subaperture imaging algorithm was proposed [4] to realize high-resolution wide-swath imaging for SAR in elliptical orbits. Various processing algorithms have been developed to deal with challenges like high squint angles [5] and time-varying parameters [6]. Accurate range models [7] and motion compensation techniques [8–10] are also critical for focusing. Moreover, some works focus on performance optimization and parameter calculation for satellites in elliptical orbits [11]. Tomographic SAR inversion [12] and challenges in

Received 8 August 2023, Accepted 16 October 2023, Scheduled 25 October 2023

* Corresponding author: Xuhang Lu (20211800129@imut.edu.cn).

[1] College of Information Engineering, Inner Mongolia University of Technology, Hohhot, China. [2] Inner Mongolia Key Laboratory of Radar Technology and Application, Hohhot, China.

advanced SAR imaging systems [13] are also related technologies. In summary, substantial efforts have been devoted to addressing the signal processing and technical difficulties associated with SAR systems in highly elliptical orbits.

High-eccentricity orbit synthetic aperture radar (HEO SAR) satellites face the formidable challenge of continuously changing orbital altitude and velocity. These fluctuations impact crucial parameters, including imaging geometry, Doppler shift, and imaging time, thus complicating the imaging processing and system design. Moreover, the radar parameters have to be precisely tailored to accommodate these geometric changes. To address these difficulties, this paper proposes an innovative method that incorporates swift variations in multiple parameters. This approach employs range-directed beam steering to ensure that the beam's center always points towards the swath's center. Further, it guarantees the accurate acquisition of echo data throughout the entire scene by adjusting the PRF and the sampling starting point. This strategy presents a viable solution to the complexities associated with HEO SAR and contributes to the refinement of SAR system design and imaging processing.

The remainder of this paper is organized as follows. Section 2 analyzes the orbital characteristics and operational challenges of HEO SAR. Section 3 proposes a multi-parameter joint agile variation system to deal with the challenges in HEO SAR. Section 4 elaborates the corresponding imaging algorithm and demonstrates it by simulations. Finally, Section 5 concludes this paper and outlines future work.

2. ORBITAL CHARACTERISTICS AND OPERATIONAL CHALLENGES OF HEO SAR

In this section, the unique orbital characteristics of HEO SAR are analyzed, and the operational challenges induced by these characteristics are discussed. First, the orbital features of HEO SAR are examined, including the high eccentricity and rapid altitude variation during each orbital period. Their impacts on SAR imaging geometry, beam pointing, Doppler parameters, and other factors are elucidated. Subsequently, the resulting challenges in echo acquisition, motion compensation, imaging processing, and system parameter design are described. By thoroughly analyzing these intrinsic properties and difficulties, effective strategies can be formulated to optimize HEO SAR operations.

2.1. Analysis of Satellite Orbital Characteristics

HEO SAR enables the satellite to possess the capabilities of both low earth orbit (LEO) and medium earth orbit (MEO) satellites. A SAR satellite in a Highly Elliptical Orbit can simultaneously provide the large-area rapid continuous imaging coverage capability of a MEO SAR satellite and the detailed sensing capability of a LEO SAR satellite in key areas, thereby significantly enhancing the differentiated observation response capability of the SAR satellite. Figure 1 illustrates three different orbital eccentricities: high eccentricity ($e = 0.4$), low eccentricity ($e = 0.05$), and circular orbit ($e = 0$).

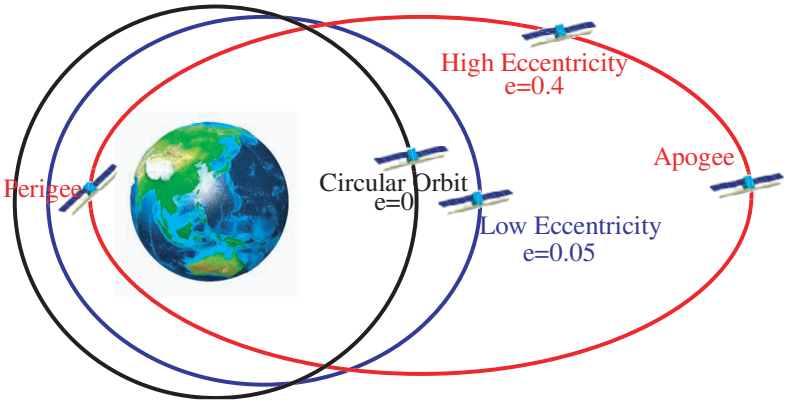

Figure 1. Comparison of satellites with different eccentricities.

For a satellite operating in a high elliptical orbit, its distance to the Earth varies periodically with its orbital position. This distance fluctuation can be characterized by the geometrical parameters of the elliptical orbit. The orbital altitude of the satellite $h(t)$ at any position can be calculated as:

$$h(t) = \frac{a(1-e^2)}{1+e\cos f(t)} \tag{1}$$

In this formula, a denotes the semi-major axis of the elliptical orbit, e the eccentricity of the elliptical orbit, and $f(t)$ the eccentric anomaly, which is the current angular position of the celestial body. According to Kepler's Second Law, as the altitude of the satellite $h(t)$ increases, the velocity of the satellite $v(t)$ correspondingly decreases:

$$v(t) = \sqrt{\mu\left(\frac{2}{h(t)} - \frac{1}{a}\right)} \tag{2}$$

Here, μ represents the Kepler constant, with a value of $3.986 \times 10^{14}\,\mathrm{m}^3/\mathrm{s}^2$ calculated as the product of the gravitational constant and the mass of the central celestial body (Earth).

Figure 2 illustrates the dynamic changes in the altitude and velocity of a satellite operating in an HEO SAR system. The parameters used in these figures are detailed in Table 1. Fig. 2(a) presents a comprehensive overview of the satellite's altitude variation throughout its entire operation. The main plot captures the overall altitude change, while the inset plot, delineated by a red box, provides a zoomed-in view of the fine-grained altitude fluctuations from the 110th to the 120th minute. This close-up inset enables careful examination of the altitude dynamics within a specific time frame. Similarly, Fig. 2(b) depicts the temporal evolution of the satellite's velocity over the same period. The main plot exhibits the velocity variation across the whole operation, whereas the inset outlined in red focuses on the velocity fluctuations during the 110th to 120th minute time window.

Table 1. Simulation parameters.

Parameter	Value
Semi-major Axis (km)	17528
Argument of Perigee (°)	270
Orbit Period (s)	21,600
Eccentricity	0.37
Inclination	63.2
Pulse Width (μs)	20
Signal Bandwidth (MHz)	300
Sampling Frequency (MHz)	360
Antenna Length (m)	5.6
Wavelength (m)	0.03

2.2. Challenges in HEO SAR Operations

The geometric model of traditional HEO SAR is depicted in Figure 3. It is evident that HEO SAR induces significant variations in parameters such as satellite altitude and velocity throughout the entire imaging process. Subsequently, three primary issues that may arise under these circumstances will be discussed: Firstly, under constant look angle, the imaging strip will become misaligned with ground swath as orbit changes, resulting in only peripheral areas being illuminated while missing the center region. Secondly, the continuous change in satellite velocity leads to alterations in the sampling interval, thereby causing the issue of nonuniform sampling in the azimuth direction. Lastly, as the satellite altitude changes, the phenomenon of range migration becomes more pronounced. These issues can degrade image quality by causing problems like swath-ground mismatch, invalid data, and defocusing.

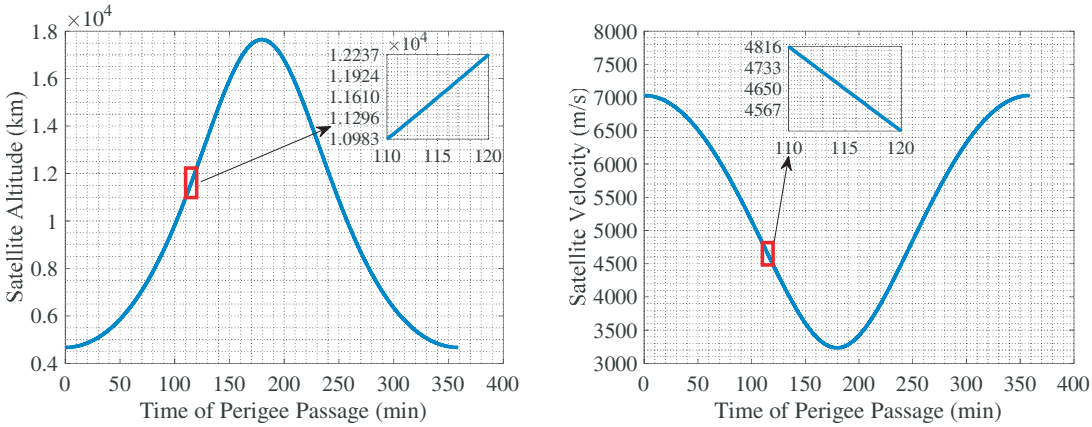

(a) Altitude of the Satellite over Time (b) Velocity of the Satellite over Time

Figure 2. Satellite dynamics over time.

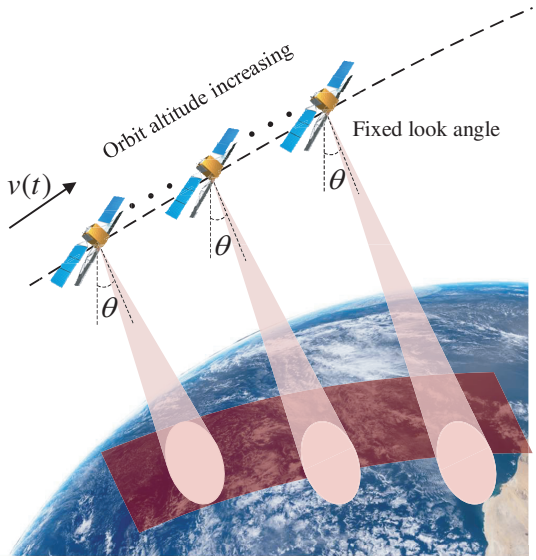

Figure 3. Imaging geometry of traditional HEO SAR.

To realize high-performance HEO-SAR imaging, effective solutions must be developed to address these challenges.

Figure 4 illustrates the time-varying echo position within the echo window of HEO SAR. It can be observed that a considerable portion of the echo window, depicted in grey, is occupied by invalid data. This invalid echo area is caused by range migration due to satellite motion variation and fixed PRF sampling mismatch. Specifically, the continuous fluctuations in altitude and velocity inherent to HEO orbits lead to substantial range migration of the SAR echo as well as nonuniform sampling in azimuth when using a fixed PRF.

Figure 5 clearly illustrates the occurrence of nonuniform sampling in HEO SAR. This irregular distribution primarily arises from the continuous fluctuations in satellite altitude and velocity inherent to high elliptical orbits. The changing altitude induces substantial range migration of the echo signal over time. Coupled with a fixed PRF, this migration leads to irregular sampling in azimuth. The resultant nonuniform sampling can cause severe image distortion and degradation, posing difficulties for data interpretation.

In summary, the unique dynamics of HEO in high elliptical orbits pose considerable challenges to SAR imaging. The significant variations in satellite state lead to issues including ground-swath

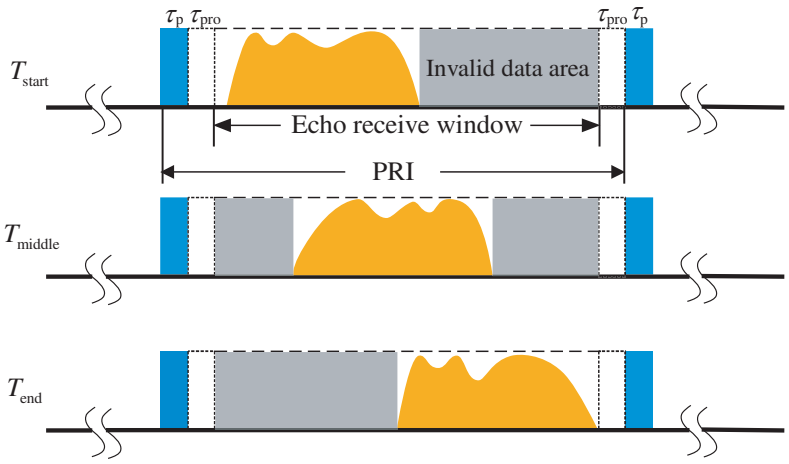

Figure 4. The variation of the satellite's echo window over time.

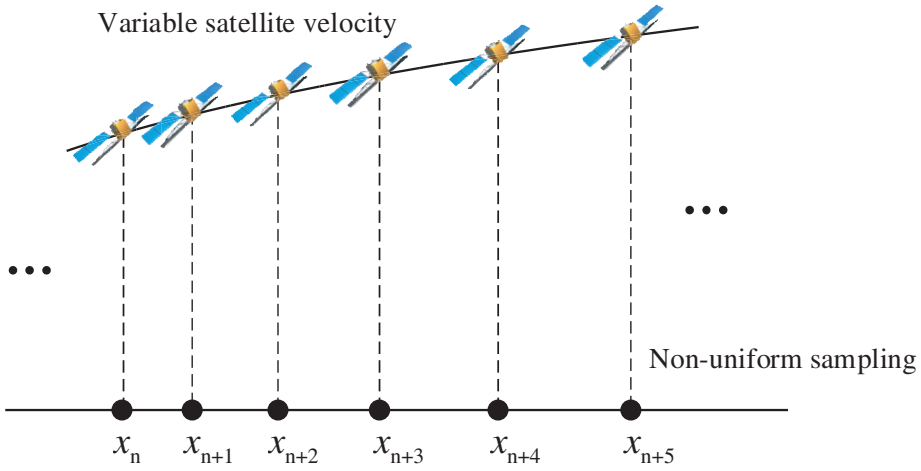

Figure 5. Sampling patterns of HEO SAR.

mismatch, irregular azimuth sampling, and excessive invalid data. Therefore, fully analyzing and effectively mitigating these issues is crucial for realizing high-resolution wide-swath SAR imaging from these distinctive orbits. Advanced solutions must be developed to overcome these challenges and unlock the potential of HEO SAR.

3. MULTI-PARAMETER JOINT AGILE VARIATION SYSTEM IN HEO SAR

Within the framework of the HEO SAR system, the joint agility of multiple parameters plays a pivotal role in determining image quality. This section will delve into the intricacies of the system's design and the methodologies employed for imaging.

3.1. System Design

Figure 6 introduces a multi-parameter joint agile variation system, an innovative mode specifically designed for HEO SAR. This system is developed to address the challenges encountered in traditional modes, particularly the issue of nonuniform azimuth sampling. The core concept of this system lies in its ability to adapt to the satellite's motion variations by simultaneously adjusting multiple parameters. These parameters include the satellite's altitude, velocity, radar scanning angle, and pulse repetition

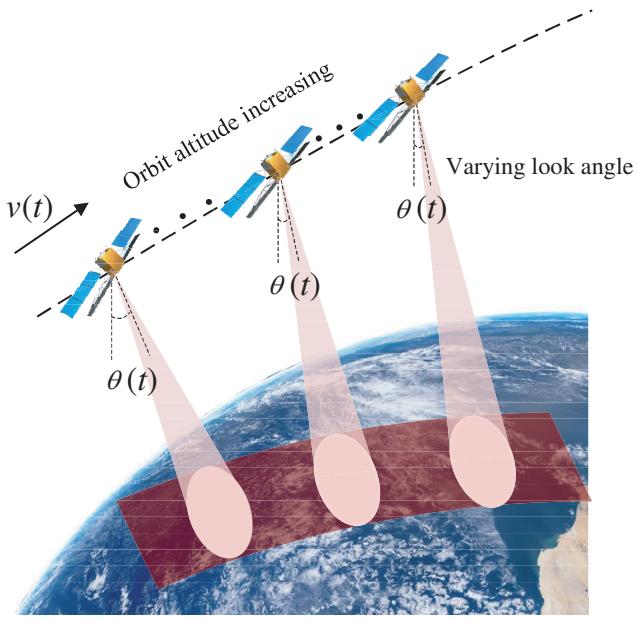

Figure 6. Imaging geometry of the proposed HEO SAR.

frequency (PRF).

By ensuring that the radar signal sampling is consistently aligned with the satellite's velocity, the system maintains the uniformity of radar signal sampling. Furthermore, the distance-oriented beam scanning angle in this mode is designed to vary with time, effectively aligning the mapping swath, or the imaging strip, with the imaging area. Dynamically adjusting the beam scanning angle to align with the imaged area as the satellite's position varies ensures that the mapping swath stays parallel to the ground through the imaging process. Maintaining this alignment minimizes geometric distortions from range migration, as the beam maintains a constant orientation relative to the imaging area despite the satellite's motion.

To achieve the alignment of the mapping strip and the imaging area in a HEO SAR system, a novel approach has been adopted, which is predicated on the precise determination of the distance-oriented beam steering variation law according to the position of the imaging mapping strip. The distance-oriented beam scanning angle is computed using the following formula:

$$\theta(t) = \arctan\left\{\frac{R_e \cdot \sin\beta}{[h(t) + R_e] - R_e \cdot \cos\beta}\right\} \tag{3}$$

where β represents the geocentric angle, and R_e denotes the Earth's radius. This method of calculating the beam scanning angle ensures that the beam direction is always optimally aligned with the mapping strip, thereby maximizing the efficiency and accuracy of the imaging process.

In addition, a design for the time-agile variation rule of the PRF has been implemented. Given the continuous variations in velocity and altitude inherent to HEO SAR, the PRF also exhibits temporal changes. To ensure consistent and high-quality sampling of the echo signal, a threshold value η is established to constrain the PRF variations within an acceptable range, typically set between 5% and 20% of the initial PRF value. If the change in $PRF(t)$ exceeds this threshold η, it is reset to its initial value PRF_0. This resetting operation serves two purposes: 1) It maintains the echo consistently within the echo window throughout the imaging process for efficient data acquisition. 2) It also contributes to mitigating the phenomenon of range migration by periodically restoring the PRF. Overall, the introduction of the threshold and resetting approach enables robust and uniform sampling of the echo signal despite significant fluctuations in velocity and altitude over the HEO orbit.

$$PRF(t) = PRF_0\left[1 + b\frac{\Delta v}{v(t_0) + (n-1)\Delta v}\right] \tag{4}$$

where b serves as a critical determinant, dictating the direction of velocity change, whether positive or negative. Δv represents the velocity variation within each PRF change sequence, while $v(t_0)$ corresponds to the velocity at the initial moment. PRF_0 represents the initial PRF value at the starting time. n serves as the sequence parameter, indicating the nth PRF change sequence, thereby providing a clear index for tracking the progression of the sequences. If $PRF(t)$ satisfies the following condition:

$$\frac{|PRF(t) - PRF_0|}{PRF_0} \geq \eta \tag{5}$$

then the variation of $PRF(t)$ exceeds the set threshold η, and it is reset to its initial value, PRF_0. This process is repeated throughout the imaging period to ensure high quality and consistency of radar signal sampling.

$$\Delta N(t) = \frac{2 \cdot f_s \cdot [r_{far}(t) - r_{near}(t)]}{c} + \frac{c \cdot f_s \cdot T_p}{2} + \Delta N_{add} \tag{6}$$

where T_p stands for the pulse width, f_s the sampling frequency, and ΔN_{add} the additional number of sampling points, typically 256 points.

To accommodate the variations in the radar echoes, a design that adjusts the start of radar echo sampling and the number of sampling points has been proposed. This design is aimed at enhancing sampling precision and reducing the demands on the satellite's storage and transmission systems. The formulas for the start of sampling $\tau_{st}(t)$ and the number of sampling points $\Delta N(t)$ are as follows:

$$\tau_{st}(t) = \text{mod}\left[\frac{2r_{near}(t)}{c}, \frac{1}{PRF(t)}\right] \tag{7}$$

where $r_{near}(t)$ and $r_{far}(t)$ represent the slant range at the near end and far end, respectively.

Figure 7 illustrates an effective approach to tackling the nonuniform sampling issue in HEO SAR. The core idea is to dynamically regulate the echo sampling start time and sampling points according to the satellite's operation time. Specifically, the number of range samples $\Delta N(t)$ is continuously updated to match the changing slant range. Meanwhile, the sampling start time $\tau_{st}(t)$ is adjusted in real-time to ensure consistent sampling intervals. Through the joint adaptation of $\Delta N(t)$ and $\tau_{st}(t)$, a uniform sampling distribution can be maintained throughout the echo acquisition process, despite significant satellite motion fluctuations. It helps eliminate excessive invalid data, concentrate echo energy, and enable easier subsequent processing. The final outcome is enhanced SAR imaging efficiency and quality from the highly dynamic HEO orbit.

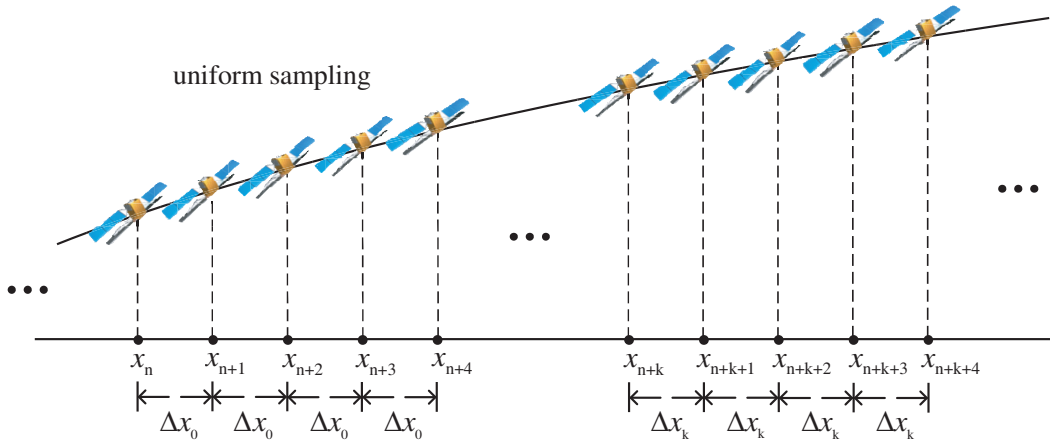

Figure 7. Addressing nonuniform sampling issues in HEO SAR.

The proposed Multi-Parameter Joint Agile Variation System presents a comprehensive solution tailored for the unique challenges of HEO SAR. By continuously monitoring the real-time satellite orbit dynamics, it precisely calculates and adjusts operating parameters including look angle, PRF, sampling points, and initiation time. Through the coordinated adaptation of these parameters, the

system maintains consistent alignment between the radar beam coverage and ground imaging swath throughout the acquisition process. This resolves the issue of swath-ground mismatch induced by varying orbits. Moreover, by regulating the sampling points and initiation time, the system compensates for irregular azimuth sampling arising from changing velocity. This technique mitigates excessive invalid data and enhances processing efficiency. In summary, the proposed system offers an effective approach to overcome the challenges posed by HEO SAR's distinctive orbital characteristics. By enabling robust imaging performance despite significant state fluctuations, this multi-parameter agile system paves the way for reliable high-resolution wide-swath HEO SAR imaging.

3.2. Imaging Processing

The algorithmic process outlined in Figure 8 comprises six essential steps.

The first step, range samples adjustment, adjusts the number of range sampling points through interpolation to account for variations in the start sampling times and numbers across different range segments. This compensates for discontinuities by converting the nonuniform samples to a uniform grid. The second step, range shift via frequency alignment, places all the interpolated range data from step one onto a consistent timeline. By aligning the uniform range samples on the same timeline, this enables easier subsequent processing of the range data. The third step, azimuth resampling, addresses the issue of nonuniform sampling in azimuth direction by performing resampling to achieve a consistent azimuth sampling rate throughout the synthetic aperture. This compensates for rotation-induced variations and ensures uniform azimuth samples for accurate frequency domain processing. The fourth step, cubic phase filtering, applies a cubic filter in the range frequency domain to eliminate cubic phase errors arising from trajectory deviation and approximations in deriving the range equation. This flattens the spectrum and improves impulse response. After filtering, the signal is transformed back to time domain to obtain the error corrected range profile [14]. The fifth step, range cell migration correction (RCMC) via range-oriented nonuniform Fourier fast transform (NUFFT), uses NUFFT to interpolate nonuniform range samples to a uniform grid, which corrects nonlinear RCMC caused by velocity variations and eliminates geometry distortions to focus the image [15]. The sixth step, azimuth compression, employs a modified matched filter in the azimuth frequency domain to account for residual range errors and cubic filtering. It focuses the azimuth by matching the azimuth frequency modulation history and recovers a well-focused image [16].

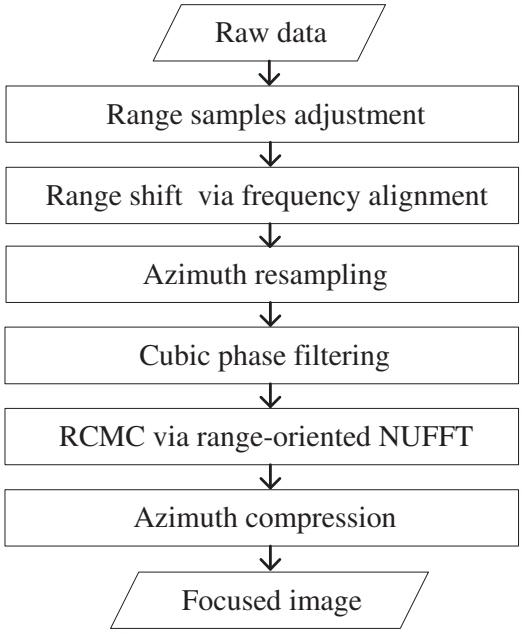

Figure 8. Flowchart of Proposed Mode Imaging Algorithm.

4. SIMULATION

In this section, a comprehensive imaging processing workflow is presented, specifically tailored to address the multi-parameter variations inherent in HEO SAR operations. This workflow, underpinned by a series of methodical steps, offers a robust solution to the challenges posed by these variations. The workflow is demonstrated using simulation parameters of an azimuth resolution of 3 m and a swath width of 30 km. Furthermore, simulation results are provided to validate the effectiveness of the proposed workflow.

4.1. Experimental Results

This section validates the effectiveness of the designed parameter calculation model through simulation. Specifically, Figure 9(a) shows the imaging angle θ gradually decreases from 33° to 25.3° between 110 and 116 minutes. This controlled steering of the look angle ensures that the radar beam is continuously aligned with the ground imaging swath center throughout the data acquisition interval. By maintaining consistent illumination coverage, it effectively addresses the issue of beam-ground mismatch induced by the changing HEO geometry. Figure 9(b) presents the variation of PRF over time. It can be observed that PRF decreases from 4180 Hz to 3860 Hz owing to changes in satellite altitude and velocity. When PRF deviation exceeds the preset threshold, PRF is promptly reset to its initial value PRF_0 to ensure uniform sampling. This thresholding technique compensates for irregular sampling arising from trajectory fluctuations. It contributes to concentrating signal energy and enhancing processing efficiency. Figures 9(c) and 9(d) illustrate the agile adaptation of sampling start time and number

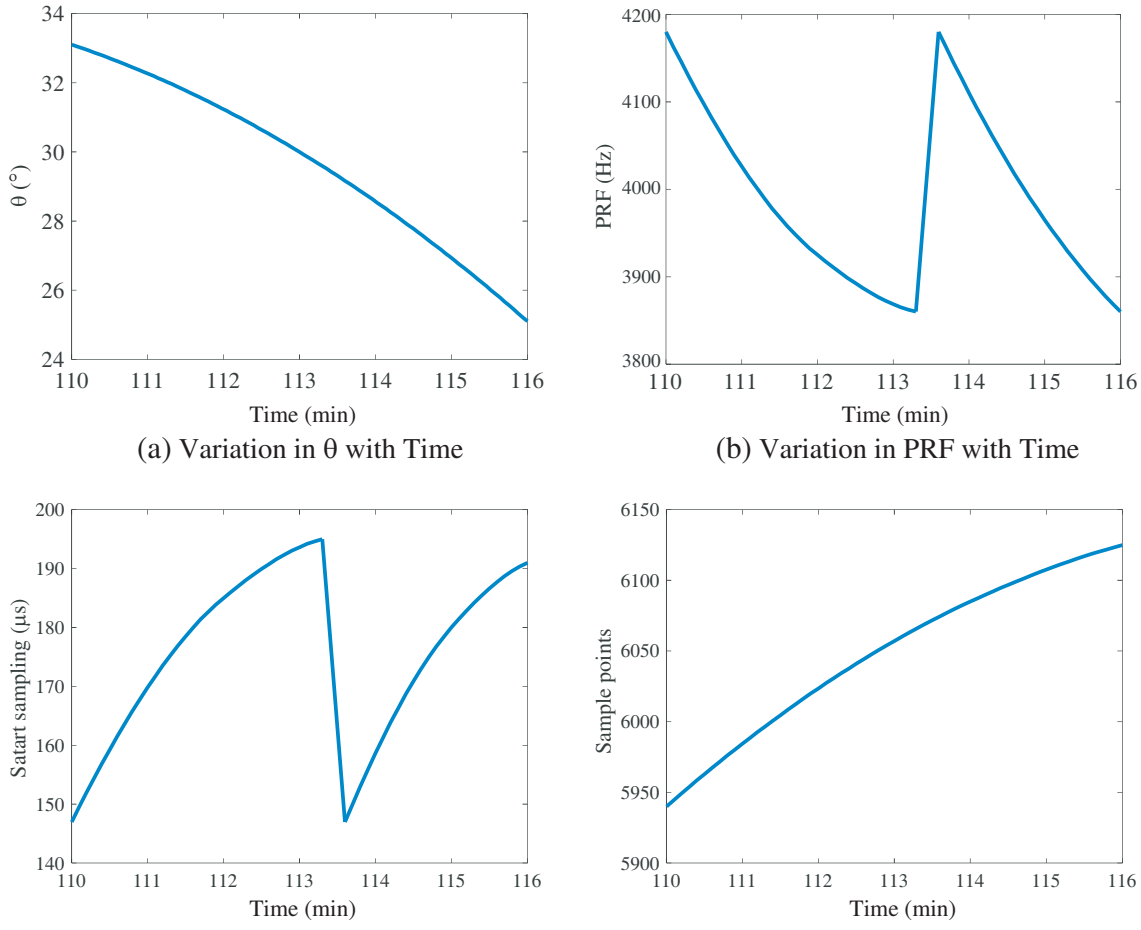

(a) Variation in θ with Time

(b) Variation in PRF with Time

(c) Variation in Start of Sampling with Time

(d) Variation in Sample Points with Tim

Figure 9. Temporal variations in key parameters.

of sampling points. The sampling start is adjusted to account for echo delay variations, while the sampling points are regulated to match the changing slant range. Through coordinated control of these two parameters, the system maintains consistent and effective sampling of the echo data despite significant motion dynamics over the HEO orbit.

4.2. Simulated Point Images

Utilizing the parameters provided in Table 1, a system design example with multi-parameters joint agile variation for the desired resolution of 3 m and the swath width of 30 km is presented. A simulation with simulated point targets spaced at 1 km in azimuth and 10 km in range is conducted to generate the image shown in Figure 10. This simulated point target image offers a clear visualization of the system's performance under the proposed algorithmic process. The simulation serves as a practical demonstration of the effectiveness of the proposed method in achieving high-quality SAR imaging. Figure 10 presents the focusing results of the proposed method, with contour plots of the three simulated point targets shown in Figures 10(b), 10(c), and 10(d). As illustrated, each simulated point target is well focused using the proposed method. Both the simulation results of multi-parameters variation design and the imaging of simulated point targets validate the proposed stripmap imaging mode with multi-parameters joint agile variation in HEO SAR. Furthermore, the resolutions of the focused point targets are quantitatively analyzed. In the azimuth direction, the resolutions of points 1, 2, and 3 are 2.93 m, 2.98 m, and 3.01 m, respectively, very close to the expected value of 3 m. In the range direction, the resolutions are 2.87 m, 2.91 m, and 2.94 m, also approximating the anticipated 3 m resolution. These quantitative results corroborate the effectiveness of the proposed imaging method in achieving the desired high resolution.

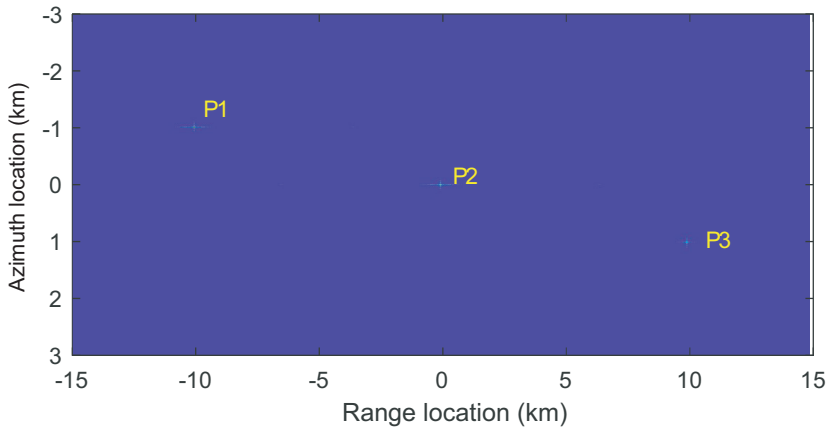

(a) Imaging result with three points

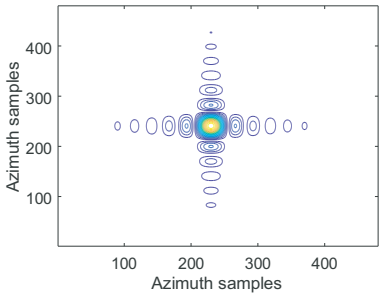

(b) Contour plots of P1

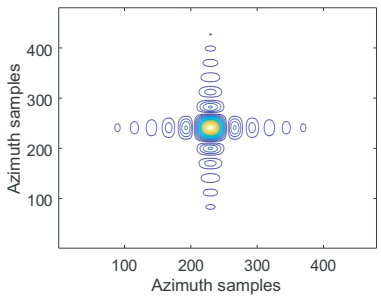

(c) Contour plots of P2

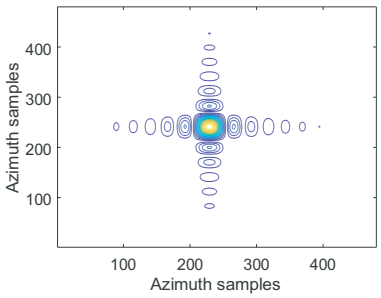

(d) Contour plots of P3

Figure 10. Point targets imaging simulation results.

5. CONCLUSION

This paper presents an innovative Multi-Parameter Joint Agile Variation System to address the challenges posed by highly dynamic HEO SAR. Due to the continuously changing altitude and velocity in HEO orbits, these variations lead to nonuniform azimuth sampling, excessive invalid data, and ground-swath mismatch. To tackle these issues, the proposed system performs real-time coordinated adaptation of multiple operating parameters, including look angle steering, PRF adjustment, and dynamic sampling point regulation. This joint control strategy ensures uniform echo sampling, efficient data acquisition, and consistent illumination throughout the data collection interval, despite significant trajectory fluctuations. Furthermore, a tailored imaging algorithm is proposed involving resampling, cubic filtering, and NUFFT to focus the non-evenly sampled HEO SAR data. Simulations validate the effectiveness of the algorithm in mitigating distortion effects. In summary, this work realizes robust high-resolution wide-swath SAR imaging from agile HEO orbits by synergistically estimating and compensating platform dynamics in real-time. The multi-parameter adaptive system and tailored algorithm provide an effective solution to overcome the challenges induced by HEO SAR's unique motion characteristics. They can be applied to enhance future HEO SAR missions' imaging capabilities and reliability. Further research directions include integrating higher-precision models and more intelligent control strategies to improve accuracy.

ACKNOWLEDGMENT

This work was supported in part by the National Natural Science Foundation of China under grant numbers 62071258, U22A2010 and 61971246.

REFERENCES

1. Zhang, Z., W. Xu, P. Huang, W. Tan, Z. Gao, and Y. Qi, "Azimuth full-aperture processing of spaceborne squint SAR data with block varying PRF," *Sensors*, Vol. 22, 9328, 2022.
2. Braun, H. M., H. Baessler, and C. Jonas, "Daily monitoring of the mediterranean sea by Geosynchronous SAR," *2016 IEEE Radar Conference*, 1–4, Philadelphia, PA, USA, 2016, doi: 10.1109/RADAR.2016.7485226.
3. Zheng, L., S. Liu, and Y. Wang, "System design of GEO-LEO bistaic SAR with high resolution and wide swath," *2018 IEEE International Conference on Mechatronics, Robotics and Automation*, 1–5, Hefei, China, 2018, doi: 10.1109/ICMRA.2018.8490564.
4. Wang, Y., R. Min, Z. Ding, T. Zeng, and L. Li, "Multi-layer overlapped subaperture algorithm for extremely-high-squint high-resolution wide-swath SAR imaging with continuously time-varying radar parameters," *Remote Sensing*, Vol. 14, No. 2, 365, 2022.
5. Hu, X., P. Wang, H. Zeng, and Y. Guo, "An improved equivalent squint range model and imaging approach for sliding spotlight SAR based on highly elliptical orbit," *Remote Sensing*, Vol. 13, No. 24, 4883, 2021.
6. Kim, A. D. and C. Tsogka, "Tunable high-resolution synthetic aperture radar imaging," *Radio Science*, Vol. 57, No. 11, e2022RS007572, 2022.
7. Sung, J.-B. and S.-Y. Hong, "In-orbit operational parameter calculation and performance optimization in KOMPSAT-6 synthetic aperture radar," *Remote Sensing*, Vol. 13, 2342, 2021.
8. Dai, C., F. Tian, and Z. Suo, "Fast geolocation solution for bistatic interferometric synthetic aperture radar configuration of inclined geosynchronous transmitter with low earth orbit receivers," *IET Radar, Sonar & Navigation*, Vol. 17, No. 5, 888–898, 2023.
9. Zhu, X. X. and R. Bamler, "Very high resolution spaceborne SAR tomography in urban environment," *IEEE Transactions on Geoscience and Remote Sensing*, Vol. 48, No. 12, 4290–4308, 2010.
10. Rossi, C., F. R. Gonzalez, T. Fritz, et al., "TANDEM-X calibrated raw DEM generation," *ISPRS Journal of Photogrammetry and Remote Sensing*, Vol. 73, 12–20, 2012.

11. Ka, M.-H., P. E. G. Shimkin, A. I. Baskakov, and M. I. Babokin, "A new single-pass SAR interferometry technique with a single-antenna for terrain height measurements," *Remote Sens.*, Vol. 11, No. 9, 1070, 2019, https://doi.org/10.3390/rs11091070.
12. Zhu, X. and R. Bamler, "Tomographic SAR inversion by L1 norm regularization — The compressive sensing approach," *IEEE Transactions on Geoscience and Remote Sensing*, Vol. 48, No. 10, 3839–3846, 2012.
13. Bordoni, F., M. Rodriguez-Cassola, and G. Krieger, "Possible sources of imaging performance degradation in advanced spaceborne sar systems based on scan-on-receive," *2020 IEEE Radar Conference*, 1–4, Florence, Italy, 2020, doi: 10.1109/RadarConf2043947.2020.9266478.
14. Zhang, Y., W. Xiong, X. Dong, et al., "A location method for ground moving target with azimuth spectrum aliasing in Geosynchronous Spaceborne-Airborne Bistatic multichannel SAR," *2019 IEEE International Conference on Signal, Information and Data Processing (ICSIDP)*, 1–4, Chongqing, China, 2019, doi: 10.1109/ICSIDP47821.2019.9173271.
15. Zhao, S., Y. Deng, and R. Wang, "Imaging for high-resolution wide-swath spaceborne SAR using cubic filtering and NUFFT based on circular orbit approximation," *IEEE Transactions on Geoscience and Remote Sensing*, Vol. 55, No. 2, 787–800, Feb. 2017, doi: 10.1109/TGRS.2016.2615000.
16. Meng, D., L. Huang, X. Qiu, et al., "A novel approach to processing very-high-resolution spaceborne SAR data with severe spatial dependence," *IEEE Journal of Selected Topics in Applied Earth Observations and Remote Sensing*, Vol. 15, 7472–7482, 2022, doi: 10.1109/JSTARS.2022.3202932.